

A Non-invasive LSO-APD Blood Radioactivity Monitor for PET Imaging Studies

Sepideh Shokouhi, Sean P. Stoll, Azael Villanueva, Paul Vaska, David J. Schlyer, Craig L. Woody, Bo Yu, Paul O'Connor, Jean-Francois Pratte, Veljko Radeka, Nora Volkow, and Joanna S. Fowler.
Brookhaven National Laboratory, Upton, New York

Abstract—A study has been carried out to investigate the possibility of using a pair of LSO + APD detector arrays to obtain a non-invasive measurement of the arterial input function for use in PET. The main focus of this study was to determine the spatial resolution and sensitivity required to obtain a high quality image that would permit a precise determination of the region of interest around the wrist artery. From these data a quantitative arterial input function that has minimal interference from the tissue and vein background can be obtained. The detector arrays were operated in coincidence counting mode to obtain planar images of various phantoms to demonstrate the feasibility of the concept.

I. INTRODUCTION

A great advantage of Positron Emission Tomography (PET) is the ability to quantify physiological processes by using models and obtaining parameters related to the metabolic state of the organ being studied. These parameters may be useful in the diagnosis and characterization of diseases and the evaluation of a course of therapy. Although some semi-quantitative PET studies do not require any direct measurement of the arterial input function [1], a wide range of quantitative studies using tracer kinetic modeling demand an accurately measured input function [2][3]. The invasive withdrawal of arterial blood is considered a health risk for both patients and hospital personnel and it is not readily compatible with clinical PET applications. Several other methods have been used to obtain the arterial input function based on using the tomograph itself or an additional detector system to get an image-derived input function.

The first of these is the direct measurement of the input function using an image of a large blood vessel [4][5][6]. There are three disadvantages in trying to obtain the arterial input function from the PET data. First, the PET tomograph has a partial volume effect limited by the resolution of the tomograph, and a major artery may not be in the field of view of the tomograph when it is focused on a particular region of interest. Second, the timing resolution is often determined by the frame acquisition speed of the PET tomograph. Typically, this is on the order of 30 seconds. Therefore, the activity trace has a time resolution of 30 seconds, although samples may be taken more rapidly with less than 5 second intervals in certain situations. If the tomograph has list mode acquisition, this restriction is relieved. In order to do accurate physiological modeling, it is essential to sample the input function as frequently as possible and, as a minimum, every few seconds. Third, the exact placement of the subject in the tomograph may affect the accuracy of the input function, and getting reproducible positioning of the trunk of the body is a difficult technical problem. Moreover it is often difficult to ensure that a major artery is in the field of view.

A second method which has been used is to place a probe over a blood vessel or on the lung to obtain a continuous measure of the blood activity [7]-[10]. The main disadvantage of this method is that there is a substantial background from the surrounding tissue that must be subtracted in order to obtain the true input function. This background comes from both the surrounding tissue and the venous background, and since the counts are not being taken in coincidence, the signal to noise ratio can be quite low.

The final technique is to use a standard input function (averaged over several normal controls) to calculate the physiological parameters [11][12]. There has also been considerable interest in modeling the input function [13][14]. In this method, the shape of the input function is calculated from various parameters. However, because the shape is very dependent on individual physiological states, and the procedural variables such as injection rate, this method can lead to very inaccurate results.

All of these techniques have potential errors. The device we are developing will allow the determination of an accurate input function by measuring the blood activity with little background from the trunk of the body.

Submitted on 10 November 2002. Correspondence should be addressed to D. Schlyer, Chemistry Department Bldg 901, Brookhaven National Laboratory 11973. e-mail schlyer@bnl.gov.

S. Shokouhi sepideh@bnl.gov and A. Villanueva with the Department of Biomedical Engineering at the State University of New York at Stony Brook. S. Stoll and C. Woody, Physics Department, Brookhaven National Laboratory. P. Vaska, and N. Volkow, Medical Department, Brookhaven National Laboratory, D. Schlyer and J. Fowler, Chemistry Department, Brookhaven National Laboratory. P. O'Connor, B. Yu, J-F Pratte and V. Radeka, Instrumentation Division, Brookhaven National Laboratory.

The authors gratefully acknowledge CTI, Inc. for supplying the LSO crystals and Brookhaven National Laboratory LDRD No. 10-28 and the Department of Energy OBER Contract No. DE-AC02-98CH10886 for their support.

The goal of this project was to investigate the possibility of using an array of LSO (lutetium oxyorthosilicate) scintillation crystals with an APD (avalanche photodiode) readout device to measure the input function. A similar non-invasive technique has been used with BGO crystals, photomultipliers and lower resolution [15]. The device also used a separate device to image the artery, but with great partial volume effect inaccuracies. Presently the first LSO-based PET scanners are available [16]. LSO has a detection efficiency similar to BGO but has faster scintillation decay time. Its high stopping power allows the use of smaller crystal elements, thus improving the spatial resolution of the detector. The resolution can approach the physical limits of about 1 mm, determined by the range of positrons in tissue and the deviation from co-linearity of the positron annihilation gamma rays. This is a continuation of our work on the measurement of the input function originally using PMTs in place of the APDs. The small size of the APD array is an attractive feature when used in the limited space of the clinical scanner. The one to one correspondence between the crystal element and the APD detector is also advantageous in identifying the point of gamma conversion. Thus the small size of the APDs and the possibility of mounting many APDs closely together in an array allows the possibility of a compact multi-module detector that is not achievable with larger photomultiplier block detectors

II. EXPERIMENTAL

A. Detector Array

We have evaluated a compact dual detector system consisting of LSO crystals and an avalanche photodiode array. Each detector module consists of thirty two $2 \times 2 \times 10$ mm³ LSO crystals in a 4×8 array, which were one-to-one coupled to a two dimensional APD array (Hamamatsu APD 8550) using a thin layer of silicone RTV. (See Figure 1)

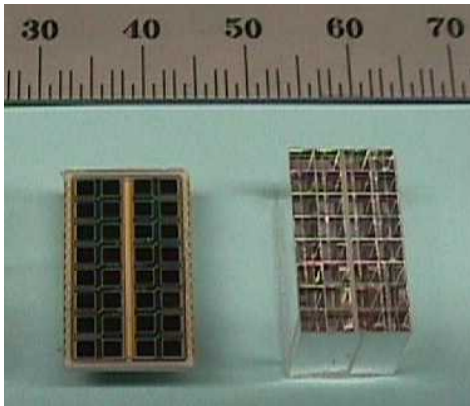


Figure 1: LSO-APD array used for measurement of input function

The APD signals were fed into a charge sensitive preamplifier and then into shaping amplifiers with a 70 ns

shaping time. The output of the shaping amplifiers were split, sending half to constant fraction discriminators (LeCroy 3240) with ~ 50 mV threshold, and half to CAMAC FERA ADCs (LeCroy 4300B) which digitize the signals. NIM logic units were used to select coincidence events and generate a gate for the FERA ADCs. Data were transferred from the CAMAC crate and analyzed externally. A schematic of the experimental setup is shown in Figure 2.

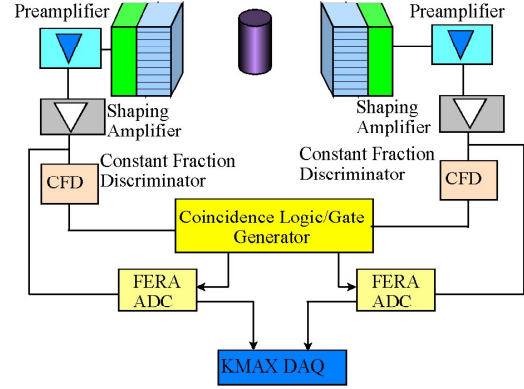


Figure 2: Experimental set up for APD array measurement.

B. Dynamic Simulations

Dynamic simulations of the input function were carried out in the following way. A 2mm internal diameter tygon tube was threaded through a peristaltic pump (Model No. Masterflex C/L model 77120-70 200 RPM) and the tubing then passed between the detectors along the long axis of the crystal arrays. The input to the pump was equipped with a 3-way valve so that the pump could be switched between a reservoir containing a solution of C-11 labeled carbonate solution and a reservoir containing pure water. A schematic diagram of this setup is shown in Figure 3.

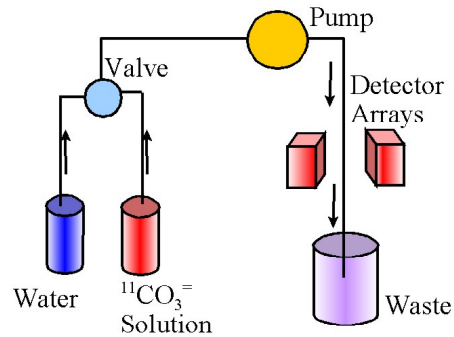


Figure 3. Schematic diagram of the dynamic phantom apparatus. Either water or a dilute $[^{11}\text{C}]\text{CO}_3^-$ solution was pumped between the detectors.

The concentration of the radioactivity flowing through the tubing was higher than normal for an arterial input function. For example the peak radioactivity concentration in blood plasma in low activity FDG study is 500 nCi/cc. The tubing length exposed to the detector surfaces is 1.6 cm. Therefore the volume of the tubing in the field of view is 0.05 cc and the activity in the field of view is approximately 25 nCi.

C. Attenuation Effects

In order to determine the effect of an attenuation medium on the sensitivity of the detector array, a lucite block was prepared which had a hole in the center just large enough to accommodate the tygon tubing. The lucite block was 4.5 cm in thickness to approximate the thickness of the human wrist. The tube was run through this block and then the block was placed between the detector arrays. After the block was placed between the detectors, a series of simulated input functions was obtained. The block was then removed and similar data acquired again. The difference between the two configurations was only a result of the lucite block since all other parameters remained the same.

D. Simulations of Arterial Input Functions

Simulations were carried out using the estimates of the noise in the data established from the typical count rates in the dynamic phantom experiments. The purpose was to determine what error was introduced by using the somewhat noisier data that we expect from the wrist detector when compared to the samples taken by the automatic blood sampling device. We chose FDG as a test case since this is the most widely used tracer in clinical PET. It is also a case where the patient may not always tolerate the procedures necessary to draw blood samples. In these experiments, an actual blood curve obtained using the automatic blood sampling device was used to calculate the global glucose metabolic value for a study carried out on a subject who had undergone a quantitative PET FDG brain study. Noise based on the expected uncertainties as determined in the experimental measurement of the count rates was then added to the blood curve using a random noise generator. The simulated blood curves were used as the input to the CTI software based on the Skoloff model and new metabolic values were calculated. These new values were then compared to the value obtained with the original blood curve.

III. RESULTS

A. Energy Resolution

The results from the energy resolution study of the detector array are shown in Figure 4. The combination of the LSO crystals and APDs produced a signal of ~ 3500 primary photoelectrons per MeV, and gave an energy resolution ~ 15 -20% (FWHM) for 511 keV gamma rays. The APD array provided an average gain of ~ 50 at a bias voltage of ~ 375 V, which resulted in a signal to noise ratio better than 50:1.

Differences in the gain of individual channels causes a shifting in their pulse height spectra. This was corrected for in the analysis of the data, where the peak position of the photopeak in each channel was shifted to the average peak position of the 32 channels in each array. This makes it more convenient to set a threshold such that only photopeak events are used for the image.

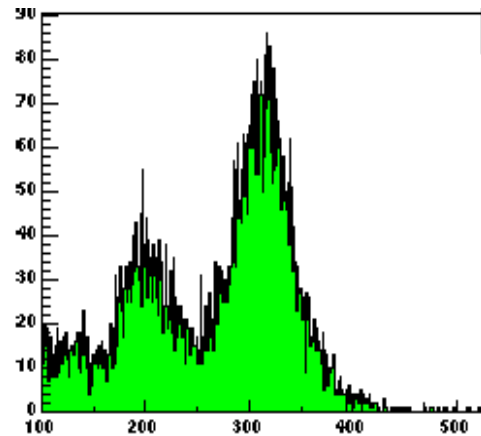


Figure 4 Pulse height spectrum for the 511 keV gamma rays from fluorine-18.

B. Sensitivity

The absolute concentration of radioactivity in the tubing was determined in a separate measurement using a calibrated NaI(Tl) well counter. The sensitivity of the detector array was determined using this known level of activity in the dynamic phantom. An estimate of this sensitivity was also calculated for the volume of activity in the field of view of the detectors (0.05cm³) and compared to the measured value. From purely geometrical arguments, it can be shown that the two detectors subtend about 11% of the azimuthal angle around the line source at a distance of 4.5 cm between the detectors. The average efficiency in the axial direction was estimated to be 0.5. In addition, there is an efficiency of ~ 0.6 for the probability for a 511 keV photon to interact in the 10 mm LSO crystals and an efficiency for triggering our coincidence circuit of ~ 0.4 . The trigger efficiency is based on the trigger threshold used in the readout electronics (~ 200 keV) and our estimate of edge effects and the effect of inter-crystal scatter in the crystal arrays on the trigger efficiency. This gives a combined efficiency of $0.6 \cdot 0.4 = 0.24$ for each gamma ray, and overall detection efficiency of $(0.11) \cdot (0.5) \cdot (0.24)^2 = 0.003$. With 25 nCi in the field of view of the detectors, this gives an estimated coincidence counting rate of 2.8 Hz, or 0.11 Hz/nCi. The measured count rate was 42 Hz with a concentration of 465 nCi in the field of view, or 0.09 Hz/nCi, which is in reasonably good agreement with our estimate. The expected count rate is

low with this sensitivity but can be increased by integrating over several seconds as is done with the automatic blood sampling machine currently in use. It should be noted that this sensitivity is for a single pair of detectors, and can easily be increased by a substantial factor by increasing the number of detectors given our current design using APDs.

C. Attenuation Experiments

The results from these experiments are shown in Figure 5. The attenuation medium had a 27% reduction in the sensitivity of the measurement. The sensitivity with the attenuation was 47.7 ± 6.3 cps as compared to 65.2 ± 7 cps without the attenuation phantom.

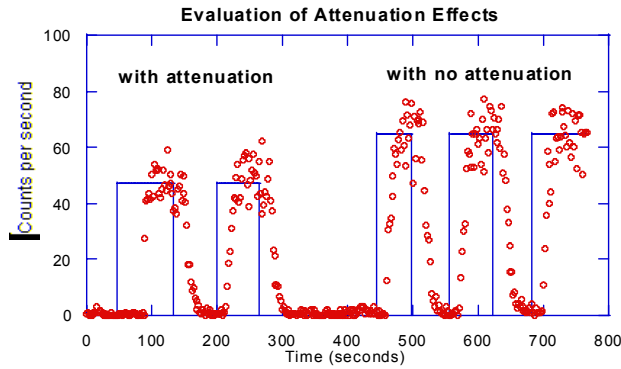


Figure 5 shows a graph of the dynamic input experiment. The data points are shown as circles while the actual activity level being pumped through is shown with the solid lines. The lag between the activity input and the response is a result of the length of tubing between the pump and the detector.

D. Image Acquisition

The planar image of the source is helpful to estimate the sensitivity and the uniformity of the block-detector system experimentally. The image of the dynamic phantom is shown in Figure 6.

Here the activity was allowed to decay in place in the tubing to simulate an image with a long acquisition time. The image acquired over a long period of time can then be used to identify regions of interest in the wrist that can then be used to generate the input function.

E. Simulations with experimental uncertainties

Ten curves were generated based on the expected signal to noise ratio for the wrist detector. The value and standard deviation obtained for whole brain metabolism were 37.74 ± 1.04 (Value \pm SD) mmoles/100 gram tissue/min., or about a 3% uncertainty in the glucose metabolic rate. This fits well within the 8% uncertainty typical of a clinical PET study [17]. The original blood curve used as the “gold standard” of the input function is shown in Figure 7.

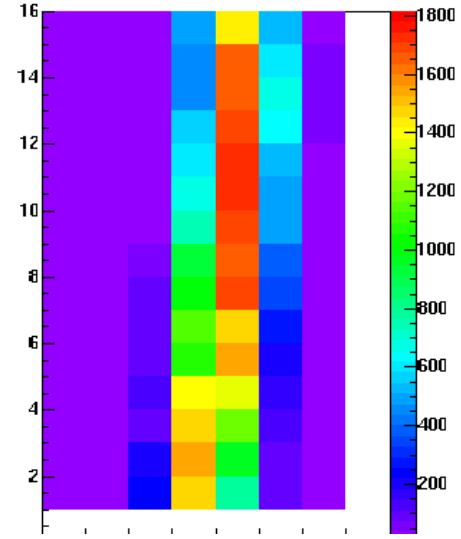


Figure 6. Two dimensional image of dynamic phantom tubing using the color scale on the right.

IV. CONCLUSIONS

The count rate sensitivity is a crucial factor in the ability to measure arterial input functions in a typical PET scan. The images obtained with this array have a good signal to noise ratio, and improvements in sensitivity by the use of several arrays along the artery should make the device capable of obtaining a good image at count rates typical of radioactivity levels in arterial blood during the first two minutes after injection. We have demonstrated that the uncertainty in the count rate is low enough that the expected error in an estimate of FDG glucose metabolic rate is less than 3 %.

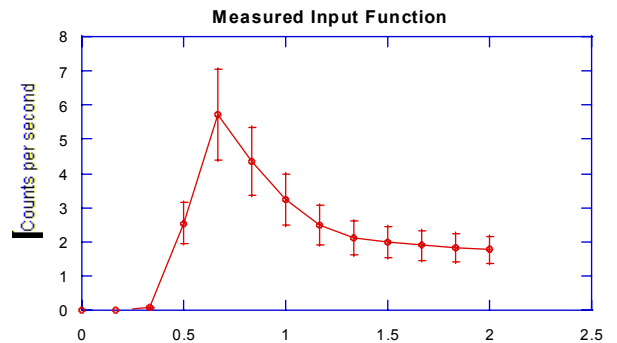


Figure 7. Input function measured using automated arterial blood sampling and the standard deviations expected based on the statistics of our counting system. The error bars are the standard deviations expected with our data.

V. ACKNOWLEDGMENT

The authors would like to express their appreciation to CTI Inc. for supplying the LSO crystals and to Proteus for constructing the arrays.

VI. REFERENCES

- [1] Logan, J., Fowler, J.S., Volkow, N.D., Wang, G-J., Ding, Y.S. and Alexoff, D.L., Distribution Volume Ratios Without Blood Sampling from Graphical Analysis of PET Data. *J. of Cerebral Blood Flow and Metabolism*, 16:834-840, 1996.
- [2] Slifstein M, Laruelle M. Models and methods for derivation of in vivo neuroreceptor parameters with PET and SPECT reversible radiotracers. *Nucl. Med. Biol.* 2001 Jul;28(5):595-608
- [3] Phelps, M.E., Huang, S.C., Hoffman, E.J., Selin, C., Sokoloff, L., and Kuhl, D.E., Tomographic Measurement of Local Cerebral Glucose Metabolic Rate in Humans with (F-18)2-Fluoro-2-Deoxy-D-Glucose: Validation of Method. *A. Neurol.* 6:371-388, 1979.
- [4] Chen, K, Bandy, D., Reiman, E., Huang, S-C, Lawson, M., Feng, D, Yun, L-S, Palant, A., Noninvasive Quantification of the Cerebral Metabolic Rate for Glucose Using Positron Emission Tomography and 18F-Fluoro-2-Deoxyglucose, the Patlak Method, and an Image-Derived Input Function. *J. Cereb. Blood Flow and Metab.* 18, 716-723, 1998
- [5] Feng, D, Wong, K.P., Wu, C.H., and Siu, W.C., A Technique for Extracting Physiological Parameters and the Required Input Function Simultaneously from PET Image Measurements: Theory and Simulation Study. *IEEE Trans. Information Technology in Biomedicine.* 4, 243-254, 1997.
- [6] Ohtake, T., Kosaka, N., Yokoyama, I., Moritan, T., Masuo, M., Iizuka, M., Kozeni, K., Momose, T., Oku, S., Nishikawa, J., Sasaki, Y., and Iio M., Noninvasive Method to Obtain Input Function for Measuring Tissue Glucose Utilization of Thoracic and Abdominal Organs, *J. Nucl. Med.*, 32 1432-1438, 1991.
- [7] Litton, J.E., and Eriksson, L., Transcutaneous Measurements of the Arterial Input Function in Positron Emission Tomography. *IEEE Trans. on Nuclear Science*, 37 627-628, 1990.
- [8] Nelson, A.D., Miraldi, F., Muzic, R.F., Leisure, G.P., and Semple, W.E., Noninvasive Arterial Monitor for Quantitative Oxygen-15 Water Blood Flow Studies, *J. Nucl. Med.* 34 1000-1006, 1993.
- [9] H. Watabe, M. Miyake, Y. Narita, T. Nakamura, M. Itoh, Development of Skin Surface Radiation detector system to monitor radioactivity in arterial blood along with Positron Emission Tomography, *IEEE Trans Nucl Sci.* 1995 42(4) 1455-1459.
- [10] M. Aykac, R.D. Hichwa , G.L. Watkins. Investigation of a noninvasive detector system for Quantitative [O-15] water Blood Flow Studies in PET. *IEEE Transactions on Nuclear Science*, VOL. 48 NO. 1 Feb. 2001 31-37.
- [11] Sadato, N., Yonekura, Y., Senda, M., Magata, Y., Iwasaki, Y., Matoba, N., Tsuchida, T. Tamaki, N., Fukuyama, H., Shibasaki, H., and Konishi, J., Noninvasive Measurement of Regional Cerebral Blood Flow Change with H215O and Positron Emission Tomography Using a Mechanical Injector and a Standard Arterial Input Function. *IEEE Trans. On Medical Imaging*, 12, 703-710, 1993.
- [12] Stritzke, P., King, M.A., Vaknine, R., and Goldsmith, S.J., Deconvolution Using Orthogonal Polynomials in Nuclear Medicine: A Method for Forming Quantitative Functional Images from Kinetic Studies. *IEEE Transactions on Medical Imaging*, 9 11-23, 1990.
- [13] Muzic, O., Behrendt, D.B., Mangner, T.J., Chugani, H.T., Design of a Pediatric Protocol for Quantitative Brain FDG Studies with PET not Requiring Invasive Blood Sampling, *J. Nucl. Med.* 35, 104P, 1994.
- [14] Wu, H.M., Hoh, C.K., Choi, Y., Schelbert, H.R., Hawkins, R.A., Phelps, M.E., and Huang, S.C., Factor Analysis for the Extraction of Blood Time Activity Curve (TAC) in Dynamic PET FDG Studies, *J. Nucl. Med.* 35, 71P, 1994.
- [15] S. Rajeswaran, D.L. Baily, Member, IEEE, S. P. Hume, D.W. Townsend, A. Geissbuehler, J. Young, T. Jones. 2-D and 3-D imaging of small animals and the human radial artery with a high resolution detector for PET. *IEEE Transactions on medical imaging*, vol. 11, no 3, Sep. 1992 385-391.
- [16] Chatzioannou, S. Cherry, Y. Shao, R.W. Silverman, K. Meadors, T.H. Farquhar, M. Pedarsani, and M.E. Phelps, Performance evaluation of microPET: a figh-resolution lutetium oxyorthosilicate PET scanner for animal imaging, *J. Nucl. Med.* 1999 40(7) 1164-1175.
- [17] Bartlett, E.J., Brodie, J.D., Wolf, A.P., Christman, D.R., Laska, E, and Meissner, M., Reproducibility of cerebral glucose metabolic measurements in resting human subjects, *J. Cereb. Blood Flow and Metab.* 1988, 8:502-512.